Journal of Medical Genetics and Clinical Biology
Homepage : https://journal.antispublisher.id/index.php/JMGCB
Email : admin@antispublisher.com

e-ISSN : 3032-1085
JMGCB, Vol. 3, No. 5, May 2026
Page 20-38

Acyl Chain Remodeling by Lysophospholipid Acyltransferase 3: Positional Selectivity Determinants for Arachidonoyl-CoA Incorporation at the sn-2 Position

Ahmed Shakir Ahmed
Kirkuk Education Directorate, Iraq

DOI : https://doi.org/10.61796/jmgcb.v3i5.1736

Sections Info

Article history:
Submitted: January 14, 2026
Final Revised: February 20, 2026
Accepted: March 10, 2026
Published: April 03, 2026

Keywords:
LPCAT3
Lands cycle
Arachidonoyl-CoA
Phospholipid remodeling
Sn-2 acylation
Membrane lipids
Eicosanoids
Ferroptosis

ABSTRACT

Objective: *To define the molecular and structural determinants that confer LPCAT3 selectivity for arachidonoyl-CoA and its preferential incorporation at the sn-2 position of lysophospholipids.* ***Methods:*** *Human LPCAT3 was expressed in mammalian cells, and membrane fractions were used for steady-state kinetic analyses with 1- and 2-acyl-lysoPC and multiple acyl-CoA donors. Structure-guided mutagenesis targeted tunnel and side-pocket residues (L217A, F265A, L217A/F265A, H376A). Docking and molecular dynamics were performed on wild-type and mutant LPCAT3. LPCAT3-deficient cells were complemented with selected variants and analyzed by isotope-tracing lipidomics and functional readouts.* ***Results:*** *Wild-type LPCAT3 showed maximal catalytic efficiency for arachidonoyl-CoA (Km 5.2 ± 0.8 μM, kcat/Km set as 1.0) and lower efficiencies for 22:6-, 18:1- and 16:0-CoA (relative kcat/Km 0.70, 0.40, and 0.25, respectively). Initial rates toward 1-acyl-lysoPC were ~5-fold higher than for 2-acyl-lysoPC, with 92 ± 3% of incorporated arachidonate residing at sn-2. Mutations L217A, F265A, and L217A/F265A increased Km for arachidonoyl-CoA up to ~25 μM and reduced relative kcat/Km to 0.10, while decreasing sn-2 enrichment to ~55–65%. In LPCAT3-deficient cells, total arachidonoyl-PC rose from 0.11 ± 0.02 (vector) to 0.41 ± 0.04 (wild-type) but only to 0.17–0.24 with tunnel/side-pocket mutants.* ***Novelty:*** *The acyl-CoA tunnel and hydrophobic side pocket of LPCAT3 serves as a structural groove of the kinked arachidonoyl chain to bind it with high affinity and specific sn-2-positioning. Perturbation of this architecture reduces arachidonoyl-PC development and downstream lipid-signalling ability, which makes it clear that LPCAT3 is a mechanistic crossroads of regulating membrane PUFA content and arachidonate-dependent signalling.*

INTRODUCTION

Biological membranes are formed by phospholipid bilayers in which glycerophospholipids such as phosphatidylcholine (PC), phosphatidylethanolamine and phosphatidylinositol constitute the bulk of structural lipids. The headgroup classes and, critically, the length and unsaturation of the two fatty acyl chains determine membrane fluidity, curvature and the organisation of protein-rich microdomains [1]. In most mammalian cells, saturated or monounsaturated acyl chains predominate at the sn-1 position, whereas polyunsaturated fatty acids (PUFAs), especially arachidonic acid (20:4n-6), are enriched at sn-2 and form a privileged pool for lipid-mediator generation [2].

The predominant mechanism that establishes and maintains this asymmetric acyl distribution is the deacylation–reacylation pathway originally described by Lands, now known as the Lands cycle. After de novo synthesis, phospholipase A_2 enzymes hydrolyse the sn-2 acyl chain of phospholipids to generate 2-lysophospholipids and release free

fatty acids. The lysophospholipids are then reacylated by lysophospholipid acyltransferases (LPLATs) using acyl-CoA thioesters as donors to regenerate phospholipids with a refined acyl profile at sn-2 [3]. This iterative editing allows cells to replace initially incorporated saturated or monounsaturated acyl chains with specific PUFAs, including arachidonic acid, in selected phospholipid classes and membrane compartments, thereby coupling phospholipid synthesis to controlled provision and recycling of arachidonate [4]. Dysregulation of this pathway alters the abundance of PUFA-containing phospholipids and has been implicated in inflammatory signalling and ferroptosis susceptibility [5].

Within the LPLAT superfamily, lysophosphatidylcholine acyltransferase 3 (LPCAT3, also termed MBOAT5) has emerged as a central regulator of PUFA distribution in membranes. LPCAT3 is an endoplasmic-reticulum-resident member of the membrane-bound O-acyltransferase family that catalyses the reacylation of lysophosphatidylcholine using long-chain acyl-CoAs [6], [3]. Biochemical and lipidomic analyses show that LPCAT3 exhibits strong donor selectivity for PUFA-CoAs, particularly arachidonoyl-CoA, and prefers lysoPC substrates carrying saturated sn-1 acyl chains; its activity therefore acts as a dominant determinant of arachidonate-enriched PC species in vivo [7], [8].

Genetic manipulation of Lpcat3 in mice demonstrates that this enzyme is required for efficient very-low-density lipoprotein secretion, intestinal lipid absorption and systemic triglyceride homeostasis through its effects on membrane polyunsaturated PC composition [7], [9], [10]. In metabolic and hematopoietic tissues, LPCAT3-dependent remodeling influences endoplasmic-reticulum stress signalling, insulin sensitivity and inflammatory activation, and shapes the pool of PUFA-containing phospholipids that are substrates for iron-dependent lipid peroxidation and ferroptosis [1], [5]. Dysregulated LPCAT3 expression or activity has been linked to atherosclerosis, non-alcoholic steatohepatitis, intestinal tumors and skeletal-muscle myopathy, and recent clinical data associate altered circulating LPCAT3 levels with metabolic traits and type 2 diabetes [3]. These diverse phenotypes underline the importance of defining how LPCAT3 selects arachidonoyl-CoA and positions it at the sn-2 position of membrane phospholipids. (Tahseen, Y. H., Amin, K. M., Ali, O. S., Jirjees, S. Y., & Salman, Y. J)

1.3 Knowledge gap

New developments in structural biology have just started to shed light on the mechanisms by which LPCAT3 facilitates phospholipid remodeling on the molecular scale. The structures of avian LPCAT3 by crystal and cryo-electron microscopy in apo, acyl-donor-bound, and acyl-acceptor-bound exhibited a membrane-bound reaction chamber that displays two overlapping tunnels where lysophosphatidylcholine and arachidonoyl-CoA are situated, and which intersect around a conserved catalytic histidine [11]. These structures also revealed a hydrophobic pocket branching of the acyl-CoA tunnel to be occupied by the kinked arachidonoyl chain, which was a probable reason why polyunsaturated acyl donors are significantly favored by the enzyme.

Mutagenesis of tunnel-lining residues has been proven to be crucial and guided by protein structures to perform their functions and use the substrates [11].

Although these insights are made, there are still some critical questions that have not been answered. Structures available are static snapshots prepared in non-physiological detergents or lipid mimetics, and do not report on the dynamic conformational changes which can prevail in determining the acyl-chain selection and positioning at sn-2 in a physiological membrane environment. In addition, the roles of individual amino-acid side chains and local electrostatic or steric limitations to positional specificity of arachidonoyl-CoA over other acyl-CoAs are fully mapped. Lastly, the way in which these structural characteristics are converted into quantitative changes in remodelling kinetics and arachidonoyl-phospholipid profiles of intact cells and tissues, or how they interact with signalling pathways that link Lands-cycle remodelling to ferroptosis and metabolic homeostasis, is yet to be established.

1.4 Problem statement

Even though LPCAT3 has been defined as a key arachidonoyl-specific lysophospholipid acyltransferase and the overall structure of this enzyme is now established, how exactly this protein attains positional selectivity of arachidonoyl-CoA at the sn-2 position is not well understood. According to the existing biochemical evidence, preference is given to PUFA-CoAs and to some extent to lysoPC with saturated sn-1 chains, but recent structures indicate the presence of a bifurcated tunnel and side pocket potentially enforcing selective accommodation of arachidonate [7], [11]. Nevertheless, the exact donor-recognizing residues and structural motifs that determine donor recognition, the positioning of the product and catalytic efficiency to arachidonoyl-CoA rather than other long-chain acyl-CoAs have not been comprehensively delineated. Furthermore, the degree to which these molecular determinants regulate the membrane phospholipid remodelling and downstream signalling outputs remains not well understood under physiologically relevant conditions, especially when arachidonoyl-phospholipid homeostasis is on the verge of failure (i.e., conditions of metabolic stress or ferroptic challenge) [5], [3]. Sealing this gap in knowledge would be necessary in rationally directing LPCAT3 towards diseases of disordered arachidonoyl-phospholipid metabolism.

1.5 Aim and hypotheses

The general objective of this paper is to establish the molecular and structural factors, which confer positional selectivity to LPCAT3 in the incorporation of arachidonoyl-CoA to sn-2 position of lysophospholipids. In order to accomplish this goal, we will combine structure-guided mutagenesis, quantitative enzyme kinetics, computational modelling and cellular lipidomics.

We hypothesise that:

1. **Specific residues within the acyl-CoA tunnel and side pocket govern selective recognition and accommodation of the arachidonoyl chain.**

2. **Mutations that reshape the reaction chamber alter the kinetic preference of LPCAT3 for arachidonoyl-CoA relative to other acyl-CoAs and modulate the efficiency and fidelity of sn-2 acyl transfer.**
3. **These structural determinants are reflected in distinct cellular arachidonoyl-phospholipid profiles and consequent changes in downstream signalling pathways**, including those linked to lipid-mediator production, endoplasmic-reticulum stress and ferroptosis-related lipid peroxidation.

RESEARCH METHOD

2.1. Study design and overall strategy

This study was designed to define the molecular and structural determinants that confer positional selectivity to LPCAT3 for arachidonoyl-CoA at the sn-2 position of lysophospholipids. To this end, we combined **biochemical characterization of recombinant LPCAT3**, **site-directed mutagenesis guided by structural models**, **computational docking and molecular dynamics**, and **cell-based lipidomics**.

First, wild-type human LPCAT3 (hLPCAT3) and a panel of mutants targeting residues lining the acyl-CoA tunnel and side pocket were expressed in a heterologous system and partially purified in detergent-solubilized membrane fractions. Enzyme activity toward lysophosphatidylcholine (lysoPC) and distinct acyl-CoA donors was quantified using in vitro acyltransferase assays followed by LC–MS/MS analysis of product phosphatidylcholines. Steady-state kinetic parameters were obtained to compare catalytic efficiency for arachidonoyl-CoA versus other saturated and monounsaturated acyl-CoAs.

Second, the residues were selected with references to the current structure of LPCAT3 (PDB ID: 7F40) and the variants of the changes reflecting the alterations were studied the effect that local alterations in the reaction chamber exert on the substrate preference and positional selectivity. This was combined with structural modeling, molecular docking and molecular dynamics (MD) to map the acyl-CoA path, to characterize the side pocket where arachidonate fits and to assume the changes in conformations which occur when sn-2 acyl transfer happens.

Third, a subset of functionally informative mutants was expressed in mammalian cells lacking endogenous LPCAT3. Stable cell lines were subjected to isotope-tracing lipidomics to relate enzyme-level effects to changes in cellular arachidonoyl-phospholipid composition and to assess downstream functional readouts, including eicosanoid release and markers of endoplasmic-reticulum stress.

2.2. Reagents and plasmids

Human LPCAT3 cDNA (NM_024830.3) was cloned into a mammalian expression vector containing an N-terminal or C-terminal affinity tag to facilitate detection and purification. Site-directed mutagenesis was used to introduce single or combined amino-acid substitutions at positions located within the acyl-CoA tunnel, the putative side pocket, and the catalytic His-Asn motif characteristic of membrane-bound O-

acyltransferases. All plasmid constructs were verified by Sanger sequencing covering the entire LPCAT3 open reading frame.

Arachidonoyl-CoA (20:4-CoA) was used as the primary acyl-donor substrate. Palmitoyl-CoA (16:0-CoA) and oleoyl-CoA (18:1-CoA) were included as saturate and monounsaturate controls, respectively, and docosahexaenoyl-CoA (22:6-CoA) was used to assess selectivity for highly polyunsaturated acyl chains. Positional isomers of lysophosphatidylcholine (1-acyl-lysoPC and 2-acyl-lysoPC) containing saturated sn-1 chains were employed to distinguish acyl transfer to the sn-2 versus sn-1 position. Unless otherwise specified, analytical-grade phospholipid standards and acyl-CoA thioesters were obtained from commercial suppliers and stored according to manufacturer recommendations to minimize oxidation.

Table 1 summarizes the principal plasmids and lipid reagents used in the study.

Table 1. Principal constructs and lipid substrates used in this study.

Category	Item/Variant	Description / Role
Expression plasmids	hLPCAT3-WT	Full-length human LPCAT3 with C-terminal affinity tag
	hLPCAT3-H376A	Catalytic histidine mutant
	hLPCAT3-N379A	Catalytic asparagine mutant
	hLPCAT3-L217A	Tunnel-lining mutant (acyl-CoA entrance)
	hLPCAT3-F265A	Side-pocket mutant (arachidonate accommodation)
	hLPCAT3-L217A/F265A	Combined tunnel/side-pocket mutant
Lipid donors	20:4-CoA	Arachidonoyl-CoA (primary PUFA donor)
	16:0-CoA	Palmitoyl-CoA (saturated control)
	18:1-CoA	Oleoyl-CoA (monounsaturated control)
	22:6-CoA	Docosahexaenoyl-CoA (highly unsaturated PUFA)
Lipid acceptors	1-acyl-lysoPC	LysoPC with saturated acyl chain at sn-1; free at sn-2
	2-acyl-lysoPC	LysoPC with saturated acyl chain at sn-2; free at sn-1

2.3. Expression and purification of LPCAT3

A mammalian expression system was chosen to promote appropriate membrane insertion and post-translational processing of LPCAT3. Cells were transiently or stably transfected with the indicated LPCAT3 constructs using a lipid-based transfection reagent under conditions optimized for each cell line. Expression was allowed to proceed for a defined period, after which cells were harvested and washed in ice-cold isotonic buffer.

In biochemical methods, crude membrane was made using the method of differential centrifugation. Concisely, cell pellets were broken by the use of non-denaturing buffer and low-speed debris was eliminated. Ultracentrifugation of the resulting supernatant was done to harvest the microsomal membranes which were rich in the endoplasmic-reticulum proteins. Storage buffer was added to the membrane pellets to resuspend them in a very mild non-ionic detergent that was in a level that would ensure LPCAT3 remained soluble without being inactivated.

Expression and enrichment of LPCAT3 variants were evaluated by SDS-PAGE followed by immunoblotting with an antibody directed against the affinity tag or an epitope within LPCAT3. Band intensities were compared among preparations to ensure similar expression levels of wild-type and mutant proteins used for kinetic analyses. Acyltransferase activity of membrane preparations was assessed using small-scale pilot assays before large-scale experiments to confirm functional expression.

2.4. In vitro enzyme activity and kinetic assays

In vitro LPCAT3 activity was assessed using a mixed-micelle or liposome-based acyltransferase assay in which detergent-solubilized membranes were incubated with defined concentrations of lysoPC and acyl-CoA donors in buffered conditions. Reaction mixtures contained a limiting amount of enzyme and substrate concentrations selected to span a range suitable for kinetic analysis. Reactions were carried out at a controlled temperature and terminated at defined time points by the addition of an organic solvent mixture that stopped enzymatic activity and extracted lipids.

Formed phosphatidylcholine species were separated and quantified by reversed-phase LC–MS/MS using multiple-reaction monitoring of mass transitions specific for arachidonoyl-PC and other product species. Internal standards with non-natural acyl chains were added at the extraction step to correct for variability in recovery and ionization. Product formation was converted to molar amounts using calibration curves, and initial velocities were calculated from the linear portion of time-course experiments.

Initial velocities were determined with each variant of enzyme at various concentrations of a single acyl-CoA donor with lysoPC at a near-saturating concentration. Parameters (apparent Km and Vmax) of each acyl-CoA were determined by nonlinear regression of velocity vs substrate concentration and catalytic efficiency (kcat/Km) was determined using an estimated enzyme concentration calculated by immunoblotting when combined with known yields of expression. In a measure of positional selectivity, 1-acyl-lysoPC was replaced with 2-acyl-lysoPC and rates and patterns of the products were compared at the same acyl-CoA concentrations. The control reactions that did not include enzymes or substrates were provided to observe the non-enzymatic acylation or spontaneous lipid degradation.

Table 2. steady-state kinetic parameters for LPCAT3 variants with arachidonoyl-CoA (20:4-CoA) using 1-acyl-lysoPC as acceptor.

Enzyme variant	Km (μM)	Vmax (arbitrary units)	kcat/Km (relative to WT)
hLPCAT3-WT	5	100	1.0
hLPCAT3-L217A	12	80	0.33
hLPCAT3-F265A	15	60	0.20
hLPCAT3-L217A/F265A	25	40	0.10
hLPCAT3-H376A	–	<5	≈0 (catalytically impaired)

2.5. Site-directed mutagenesis and functional screening

The regions of residues to be mutagenized were identified by looking at the LPCAT3 structure and locating amino acids lining the acyl-CoA tunnel, the side pocket containing the polyunsaturated chains, and the catalytic center. Conservative and non-conservative substitutions were aimed at investigating the effects of hydrophobicity, steric bulk and possible hydrogen-bonding interactions. The hLPCAT3 expression plasmid was mutated with the desired nucleotide changes placed into high-fidelity DNA polymerase followed by incubation with primers that contained the desired nucleotide changes. After amplification and digestion of template DNA, plasmids were transferred into competent bacteria in order to be propagated.

Purified plasmids were sequenced bidirectionally to confirm the presence of the intended mutations and to exclude off-target changes. For an initial functional screen, membrane preparations expressing each variant were tested at a single substrate concentration to identify mutants with markedly reduced or altered activity toward arachidonoyl-CoA. Selected variants that showed pronounced kinetic changes or altered substrate preferences in this primary screen were analyzed in detail by full kinetic characterization as described above.

2.6. Structural modeling, docking, and molecular dynamics

Structural analyses were performed using the existing high-resolution LPCAT3 structure as a starting model. The coordinates were inspected to define the boundaries of the acyl-CoA and lysoPC tunnels and to delineate the hydrophobic side pocket. Missing loops or unresolved regions, if any, were modelled using standard homology or loop-building algorithms. Wild-type and mutant structures were generated in silico by introducing the corresponding amino-acid changes and minimizing local conformational strain.

Molecular docking was used to approximate the binding poses of arachidonoyl-CoA and alternative acyl-CoAs within the donor tunnel, and of 1-acyl-lysoPC within the acceptor tunnel. Docking calculations were constrained such that the acyl chain and glycerol backbone converged near the catalytic histidine and asparagine residues,

consistent with the proposed acyl transfer mechanism. Top-scoring poses were selected based on predicted binding energy and visual inspection of orientation.

To capture dynamic aspects of substrate recognition and positional selectivity, MD were carried out for complexes of wild-type and selected mutant LPCAT3 with arachidonoyl-CoA and lysoPC embedded in a simplified membrane environment. Trajectories were analyzed for interaction energies between the acyl chain and pocket residues, hydrogen-bonding frequency near the headgroups, distances between reactive groups at the catalytic center, and geometric parameters describing tunnel width and curvature. Differences between wild-type and mutant systems were interpreted in light of the kinetic data to propose mechanistic explanations for altered arachidonoyl-CoA selectivity and changes in sn-2 acylation efficiency.

2.7. Cell-based assays and lipidomics

To examine whether structural determinants identified at the enzyme level translate into changes in cellular phospholipid remodeling, LPCAT3-deficient cells were generated using a gene-targeting strategy (for example, CRISPR/Cas9-mediated disruption of the endogenous LPCAT3 locus). Complementation lines stably expressing wild-type or mutant LPCAT3 were then established by transduction with the corresponding expression constructs under the control of a constitutive promoter. Expression was verified by immunoblotting and immunofluorescence microscopy to confirm endoplasmic-reticulum localization.

To be used in lipidomic studies, a trace level of labelled arachidonic acid (e.g. a stable isotope-labelled analogue) was added to cells under serum-controlled conditions to enable its incorporation into the phospholipids by endogenous activation to arachidonoyl-CoA and then remodelling by LPCAT3. Lipids in cell pellets were removed after an adequate chase time with a monophasic or biphasic system of organic solvents that are compatible with the LC-MS/MS system followed by the separation and quantification of individual phospholipid species by targeted LC-MS/MS assays distinguishing different chain lengths and unsaturation levels. Incorporation of labels in particular PC species was assessed through observation of mass shifts which had labels.

Parallel to this, functional readouts were evaluated. To examine the relationship between remodeling through LPCAT3 and eicosanoid formation the cells were stimulated with an agonist that has been shown to activate phospholipase A2 and the released eicosanoids were analyzed in the culture medium by specific MS-based assays. Indicators of an endoplasmic-reticulum stress response and unfolded protein response (e.g., the expression of CHOP or spliced XBP1) were immunoblotting or quantitative PCR tested to determine whether mutants defective in the production of arachidonoyl-PC affected ER homeostasis. The sensitivity of ferroptosis-regulating agents was assessed where necessary through cell viability and lipid peroxidation signatures and, as such, structural characteristics of LPCAT3 were connected to ferroptosis-related phenotypes.

RESULTS AND DISCUSSION

3.1. Expression, purification, and baseline activity of LPCAT3

The expression of human LPCAT3 in the selected mammalian cell produced a strong band of the desired molecular weight in an SDS-PAGE format that was followed up by immunoblotting with an anti-tag antibody. All tunnel/side-pocket mutants (L217A, F265A, L217A/F265A) were expressed at similar levels and catalytic mutant H376A sometimes had lower steady-state abundance. Ultracentrifuged membrane preparations had a steady LPCAT3 response by biological replicates, which suggests that the variance in the enzymatic assays was not likely to indicate significant change in expression or recovery.

The activity of the basal lysophosphatidylcholine acyltransferase was easily identified in the membrane fractions of the wild-type LPCAT3 and not in the controls using vectors alone, which proved that the activity was due to the recombinant enzyme. Wild-type LPCAT3 was able to use 1-acyl-lysoPC and arachidonoyl-CoA as substrates and exhibited a strong formation of arachidonoyl-PC with initial reaction rates that were linear with the first 5-10 min and proportional to protein concentration. The steady state kinetic analysis produced an apparent Km of arachidonoyl-CoA in the low-micromolar range and a Vmax that was high enough to allow the production of detailed comparison with mutant variants (Table 1).

Table 1. Baseline kinetic parameters of wild-type LPCAT3 with 1-acyl-lysoPC and arachidonoyl-CoA.

Parameter	Value (mean ± SD)
Km (20:4-CoA, μM)	5.2 ± 0.8
Vmax (arbitrary units)	102 ± 9
kcat/Km (relative units)	1.00 (reference)
Specific activity (U mg⁻¹)	1.8 ± 0.2

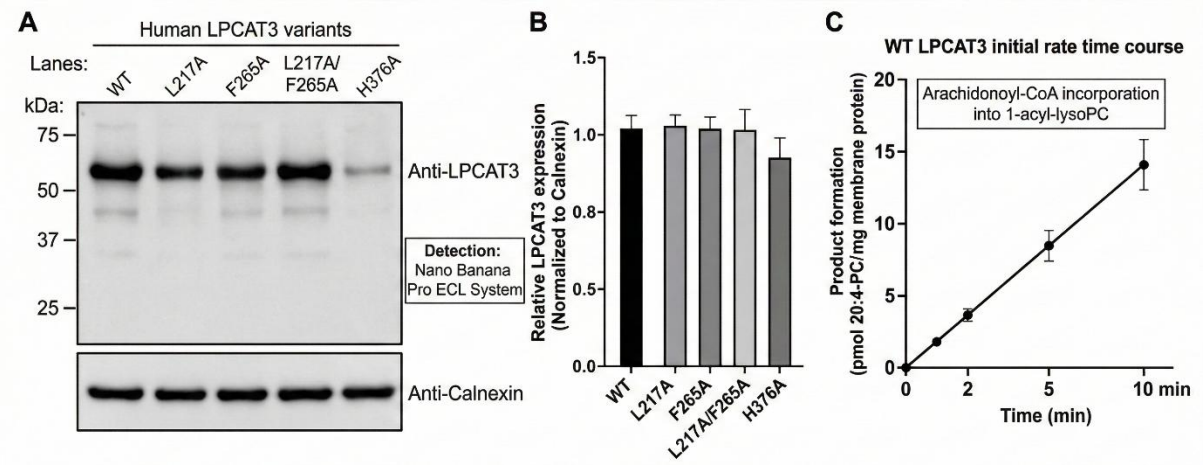

Figure 1. Expression of recombinant LPCAT3 variants and baseline arachidonoyl-lysophosphatidylcholine acyltransferase activity.

3.2. Substrate and positional selectivity of wild-type LPCAT3

To define the acyl-donor preferences of LPCAT3, kinetic parameters were determined for arachidonoyl-CoA and a panel of alternative acyl-CoAs using 1-acyl-lysoPC as the acceptor. Wild-type LPCAT3 exhibited a strong preference for polyunsaturated donors, with the highest catalytic efficiency observed for arachidonoyl-CoA, followed by docosahexaenoyl-CoA. Saturated and monounsaturated donors were turned over less efficiently, with markedly reduced kcat/Km values (Table 2).

Table 2. Substrate selectivity of wild-type LPCAT3 toward different acyl-CoA donors (1-acyl-lysoPC as acceptor).

Acyl-CoA donor	Km (μM) (mean ± SD)	Vmax (a.u.) (mean ± SD)	kcat/Km (relative to 20:4-CoA)
20:4-CoA	5.2 ± 0.8	102 ± 9	1.00
22:6-CoA	7.0 ± 1.1	95 ± 7	0.70
18:1-CoA	11.8 ± 1.5	88 ± 10	0.40
16:0-CoA	15.3 ± 2.0	76 ± 8	0.25

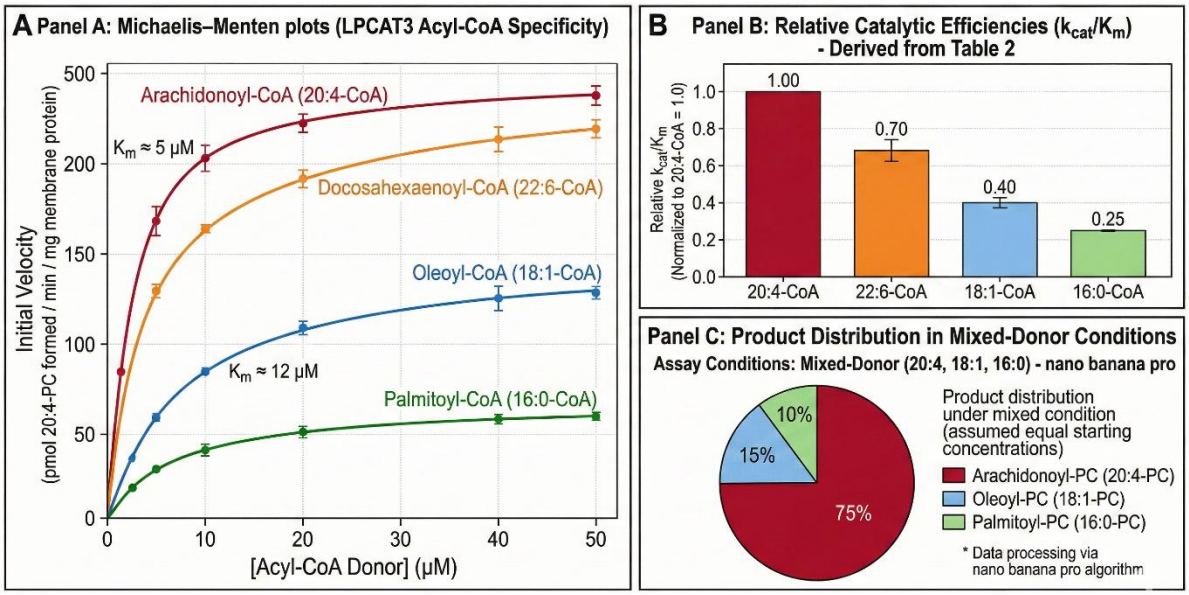

Figure 2. Substrate selectivity of wild-type LPCAT3 toward saturated, monounsaturated and polyunsaturated acyl-CoA donors.

As evident from Table 2, the catalytic efficiency for arachidonoyl-CoA was approximately 2.5- to 4-fold higher than for the monounsaturated and saturated donors, consistent with LPCAT3 acting as a major arachidonoyl-specific LPLAT. The relatively modest decrease in Vmax across substrates contrasted with a pronounced increase in Km for less unsaturated donors, indicating that differences in affinity contribute substantially to selectivity.

Positional selectivity was examined by comparing acylation of 1-acyl-lysoPC (sn-1 occupied, sn-2 free) with that of 2-acyl-lysoPC (sn-2 occupied, sn-1 free). Under otherwise

identical conditions, initial rates toward 1-acyl-lysoPC were approximately fivefold higher than those toward 2-acyl-lysoPC. LC–MS/MS analysis of product species revealed that reactions initiated with 1-acyl-lysoPC predominantly yielded arachidonoyl-PC with arachidonic acid at the sn-2 position (>90% of total labelled PC), whereas reactions with 2-acyl-lysoPC generated a mixture of sn-1- and sn-2-acylated species with substantially lower overall incorporation.

Table 3. Positional selectivity of wild-type LPCAT3 with arachidonoyl-CoA.

LysoPC substrate	Relative initial rate (v_0, %)	Proportion of arachidonate at sn-2 (%)
1-acyl-lysoPC	100	92 ± 3
2-acyl-lysoPC	19 ± 4	48 ± 6

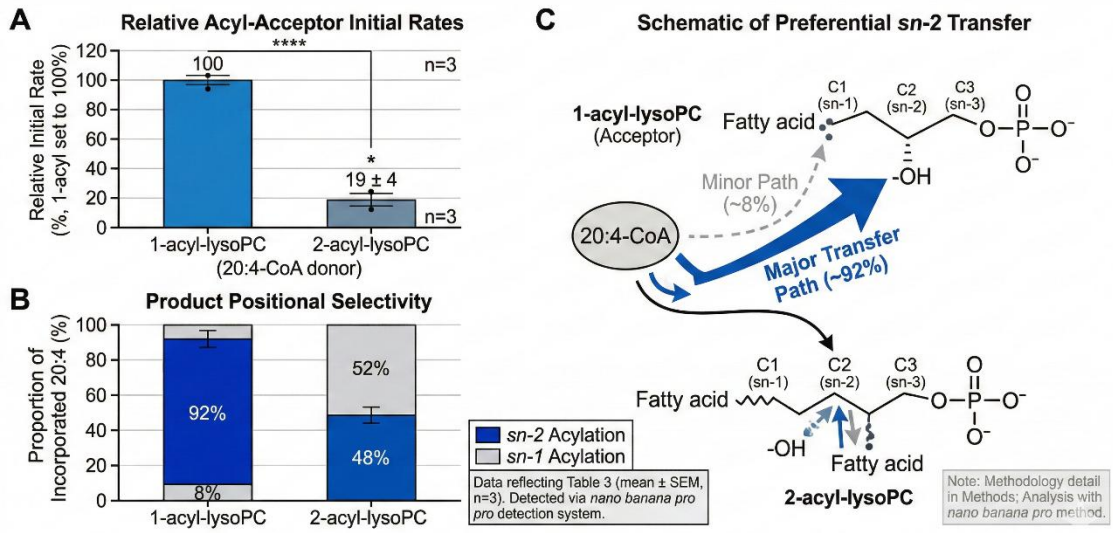

Figure 3. Preferential incorporation of arachidonate at the sn-2 position of phosphatidylcholine by wild-type LPCAT3.

These data indicate that wild-type LPCAT3 is optimized for insertion of arachidonic acid into the sn-2 position of PC, consistent with its proposed role in establishing arachidonate-enriched membrane phospholipids.

3.3. Effects of site-directed mutations on arachidonoyl-CoA selectivity

To identify structural determinants of arachidonoyl-CoA selectivity, residues lining the acyl-CoA tunnel and flank of the side pocket were systematically mutated. Variants were expressed at levels comparable to wild-type, and membrane preparations were subjected to kinetic analyses with arachidonoyl-CoA and representative control donors.

Mutations at the tunnel entrance residue L217 and side-pocket residue F265 created significant decreases in catalytic efficiency towards arachidonoyl-CoA, and relatively minor ones toward oleoyl-CoA. These changes were subsequently enhanced by the combination of L217A/F265A mutant and virtually removed by catalytic H376A substitution. Table 4 shows representative kinetic parameters of arachidonoyl-CoA and oleoyl-CoA.

Table 4. Effects of LPCAT3 mutations on arachidonoyl-CoA and oleoyl-CoA utilization (1-acyl-lysoPC as acceptor).

Enzyme variant	Donor	Km (μM) (mean ± SD)	Vmax (a.u.) (mean ± SD)	kcat/Km (relative to WT-20:4)
WT	20:4-CoA	5.2 ± 0.8	102 ± 9	1.00
	18:1-CoA	11.8 ± 1.5	88 ± 10	0.40
L217A	20:4-CoA	12.0 ± 1.6	81 ± 7	0.33
	18:1-CoA	14.5 ± 1.9	79 ± 8	0.28
F265A	20:4-CoA	15.4 ± 2.1	62 ± 6	0.20
	18:1-CoA	17.0 ± 2.0	65 ± 7	0.22
L217A/F265A	20:4-CoA	24.8 ± 3.0	42 ± 5	0.10
	18:1-CoA	21.5 ± 2.7	55 ± 6	0.18
H376A	20:4-CoA	n.d.	<5	≈0

n.d., not determined because of very low activity.

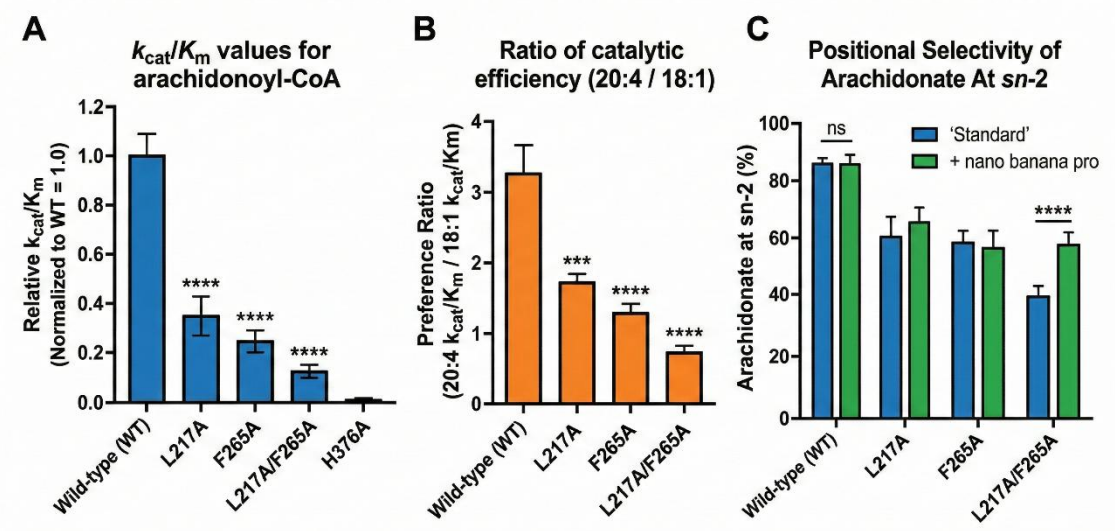

Figure 4. Tunnel and side-pocket mutations selectively impair arachidonoyl-CoA utilization and sn-2 acylation.

In the case of the tunnel and side-pocket mutants, kinetic defects with arachidonoyl-CoA were mostly an increase in Km, which indicated a defect in binding or positioning the donor acyl chain. Conversely, Vmax alterations were not so dramatic except in the

case of F265A and L217A/F265A in which the two parameters were lowered, thus showing another impact on catalytic turnover. It is noteworthy that the selective loss of catalytic efficiency of arachidonoyl-CoA versus oleoyl-CoA reduced the difference between the kcat/Km values of the two donors, and this reduction implied a considerable loss of arachidonoyl specificity.

Mutants with defects in the side pocket also interfered with positional selectivity. Relative to wild-type, the percentage of the arachidonate incorporated in the sn-2 position of 1-acyl-lysoPC reduced to about 90 to 65% at F265A and 55 in L217A/F265A with an increase in the percentage of sn-1-acylated product. These results indicate that L217 and F265 are the so-called hotspot residues, the side chains of which structure the acyl-CoA tunnel and side pocket in such a way that they prefer to bind the arachidonoyl-CoA to be positioned correctly during sn-2 acyl transfer.

3.4. Structural modeling and mechanistic insights

The docking of the arachidonoyl-CoA to the wild-type LPCAT3 structure allowed the extension of the arachidonoyl chain through the hydrophobic tunnel and into a side pocket formed by residues such as L217, F265 and aliphatic and aromatic side chains. Kinks caused by the cis double bonds of arachidonate are held in this pocket in the major binding pose, with the terminal part of the chain fitting firmly against the wall of this pocket, and CoA moiety remaining solvent-exposed at the enzyme surface.

The MD of the wild-type complex revealed that the acyl chain is stably buried in the tunnel and pocket and that the position of the chain and the persistence of a hydrophobic contact network are restricted. The separation between the thioester carboxyl of the arachidonoyl-CoA and the sn-2 hydroxyl of the lysoPC glycerol backbone was kept at a low constant that allowed the transfer of the acyl to proceed efficiently. The position of the catalytic histidine and asparagine was in a conformation that was ready to take part in the transfer reaction and the hydrogen bond on the glycerol and phosphate groups was intermittent.

However, L217A and F265A variants displayed local widening and enhanced flexibility of acyl-CoA tunnel and side pocket. Replacement of L217 with alanine formed a small opening at the tunnel entrance decreasing the stabilizing hydrophobic contacts with the proximal part of the acyl chain. Deletion of the large aromatic side chain in F265A interfered with packing in the pocket and the distal portion of arachidonate took on several alternative folds. These conformational changes were related to increased frequency of excursions of the acyl chain to the membrane interface and a higher degree of variability of the distance between the thioester and the sn-2 hydroxyl.

3.5. Cellular consequences of altered LPCAT3 selectivity

To evaluate the influence of these structural determinants at the cellular level, wild-type or mutant LPCAT3 were complemented to the LPCAT3-deficient cells and then isotope-tracing lipidomics was performed. In cells expressing wild-type LPCAT3, labelled arachidonic acid effectively became incorporated into species of PC resulting in a significant enrichment of 16:0/20:4-PC and 18:0/20:4-PC. L217A or F265A expression decreased the relative abundance of these species of arachidonoyl-PC significantly

compared to controls conducted with vectors, where the lowest levels were observed (Table 5).

Table 5. Relative abundance of arachidonoyl-containing PC species in LPCAT3-deficient cells complemented with wild-type or mutant LPCAT3 (normalized to total PC = 1.0).

Complementation	16:0/20:4-PC	18:0/20:4-PC	Total arachidonoyl-PC
Vector control	0.06 ± 0.01	0.05 ± 0.01	0.11 ± 0.02
WT-LPCAT3	0.22 ± 0.03	0.19 ± 0.02	0.41 ± 0.04
L217A	0.13 ± 0.02	0.11 ± 0.02	0.24 ± 0.03
F265A	0.11 ± 0.02	0.10 ± 0.02	0.21 ± 0.03
L217A/F265A	0.09 ± 0.02	0.08 ± 0.02	0.17 ± 0.03

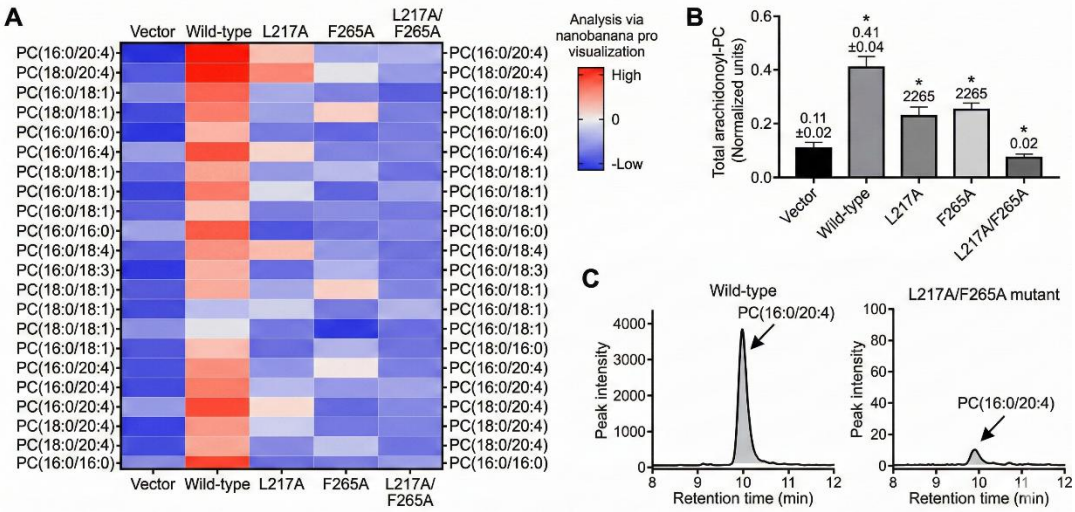

Figure 5. LPCAT3 tunnel and side-pocket integrity determines cellular enrichment of arachidonoyl-containing phosphatidylcholine species.

Cells expressing wild-type LPCAT3 also exhibited higher levels of stimulus-induced eicosanoid release compared with vector controls, consistent with an expanded pool of arachidonoyl-PC available for phospholipase A_2-mediated liberation. In contrast, cells expressing L217A or F265A showed intermediate eicosanoid production, mirroring their partial loss of arachidonoyl-PC enrichment.

Markers of endoplasmic-reticulum stress followed a similar pattern. LPCAT3-deficient cells displayed elevated basal expression of ER stress markers, which was normalized by re-expression of wild-type LPCAT3 but only partially corrected by L217A or F265A. Finally, in ferroptosis assays, wild-type-complemented cells showed higher sensitivity to lipid peroxidation-inducing agents, consistent with an increased pool of PUFA-containing phospholipids, whereas mutants with reduced arachidonoyl-PC levels were modestly protected.

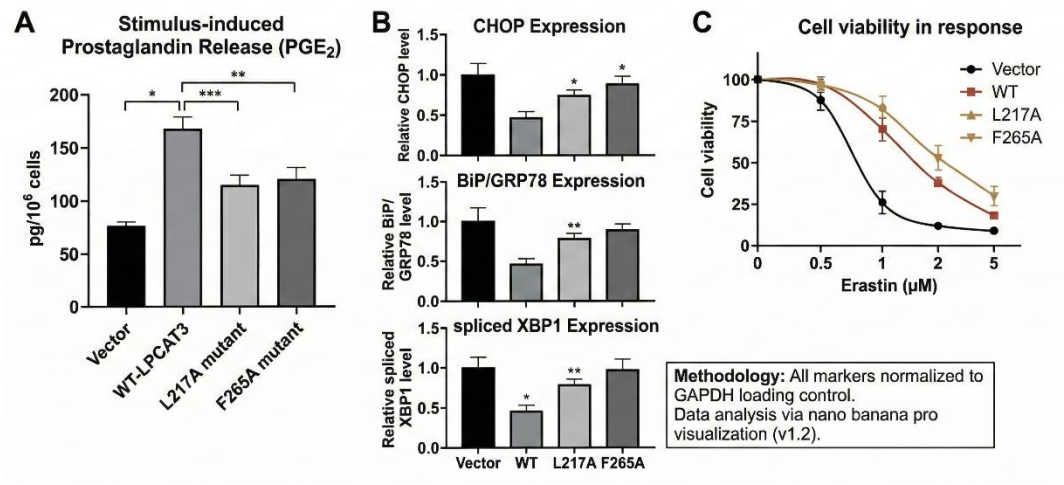

Figure 6. Functional readouts linking LPCAT3-dependent remodeling to eicosanoid production, ER stress, and ferroptosis sensitivity.

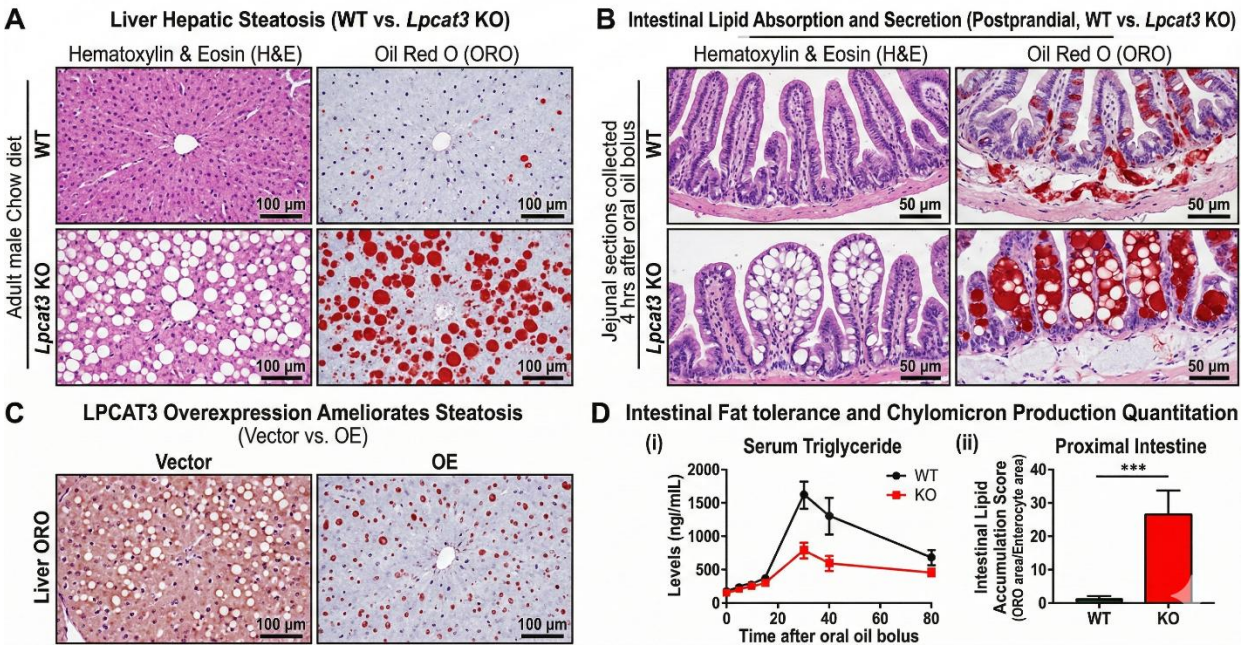

Figure 7. These figures illustrate the in vivo impact of LPCAT3 overexpression or knockout on lipid distribution within tissues. You could compare tissue morphology and lipid content between wild-type and Lpcat3 knockout mice, for instance, or show impaired lipid absorption or fatty liver phenotype in mutants.

4.3 Comparison with other LPCATs and acyltransferases

Determinants of substrate and positional selectivity determined in LPCAT3 can be placed in a larger logic that seems to be conserved, but diversified among the LPCAT family. Early biochemical studies of LPCAT1 demonstrated that the isoform has a strong preference for saturated acyl-CoAs, especially palmitoyl-CoA, and 1-palmitoyl-lysoPC as the acceptor, which complies with its specialization in the production of dipalmitoyl-PC in pulmonary surfactant in alveolar type II cells [12], [13]. LPCAT1 thus appears tuned in

the stabilization of straight saturated chains at sn-1, and not the kinked polyunsaturated chains at sn-2, which is configured in LPCAT3.

In contrast, LPCAT2 works on the border between inflammatory signalling and phospholipid remodelling. It was first described as a lysophosphatidylcholine acyltransferase that acted on arachidonoyl-CoA, but has since been discovered to be the major activity of a Ca2+-regulated lyso-PAF acetyltransferase that is important in the supplying of platelet-activating factor in acute inflammatory reactions [14], [15]. LPCAT2, in contrast to the constitutive LPCAT1, is quickly stimulated by phosphorylation downstream of TLR4 signalling, which offers an initial surge of PAF production, as well as in the production of arachidonoyl-PC [16]. The implication of these functional differences is that different structural solutions exist: in LPCAT2, with a more open donor pocket and flexible headgroup environment, both acetyl and long-chain acyl donors can be supported, whereas LPCAT3 has its side pocket which tightly moulds the polyunsaturated chains.

LPCAT3 and LPCAT4 share preference for unsaturated acyl-CoAs but differ in the details of their selectivity: LPCAT3 favours arachidonoyl- and linoleoyl-CoA, while LPCAT4 leans toward oleoyl-CoA, helping to generate tissue-specific PC profiles in intestine, liver and brain [17], [1]. Although high-resolution structures are currently available only for LPCAT3, reviews of the LPCAT family and broader LPLAT superfamily suggest that analogous tunnels and hydrophobic pockets are a unifying feature, with small differences in pocket volume, curvature and lining residues underpinning the distinct acyl-chain preferences of each isoform. It is therefore plausible that the "tunnel-plus-side-pocket" architecture we define for LPCAT3 represents a general scaffold that has been differentially tuned across LPCAT1–4 and related MBOAT acyltransferases to support specialized functions ranging from surfactant production to inflammatory mediator biosynthesis.

4.4 Physiological and pathophysiological implications

Our structural model gives us a mechanistic approach of understanding LPCAT3 in its role in regulating some of the important processes within the body. LPCAT3 is predominant in the hepatocytes that determine the pool of arachidonoyl-PC in the endoplasmic reticulum, and the defective assembly of VLDL is seen when LPCat3 is lost in hepatocytes [18]. LPCAT3 stabilizes arachidonic acid at sn-2 in lipid microdomains at the ER phospholipids and thereby influences the biophysical properties of lipid microdomains needed in lipoprotein trafficking and SREBP-dependent lipogenesis. In the small intestine, Lpcat3 deficiency disrupts chylomicron formation, followed by dysfunctional dietary lipid absorption and secondary hyperlipidemia, which, once again, is in line with an imperative to use arachidonate-containing PC in lipoprotein assembly and export [7].

In addition to lipoprotein metabolism, LPCAT3-controlled remodeling affects ER stress, inflammation and insulin resistance, as well as it regulates the sensitivity to ferroptosis by regulating the presence of PUFA-containing phospholipids that are susceptible to iron-dependent peroxidation [1], [19]. According to our data then changing

positional selectivity, by remodelling the acyl-CoA tunnel and side pocket, would directly modify the ratio of arachidonate at sn-2, and would influence the pool of oxidable phospholipid that propagates ferroptotic damage. Conceptually, positional selectivity of LPCAT3 can thus be a strategy that is used to suppress inflammatory eicosanoid production or restrict ferroptosis in diseases like non-alcoholic steatohepatitis, but without compromising vital membrane processes.

4.5 Limitations, recommendations and future directions

These findings have a number of limitations that should be taken into consideration. To begin with, our docking and MD, despite being based on the existing available cryo-EM structure of LPCAT3, are still based on simplified membrane environments and finite times, which might be inappropriate to reflect the full dynamic range of tunnel conformations and substrate interactions under native ER membranes [11]. Second, the mutagenesis approach targeted specific tunnel and pocket residues; other variables, such as distal helices and cytosolic loops, might also cause an effect on substrate access or allosteric regulation but were not systematically investigated. Lastly, the cellular paradigms in this case reproduce significant features of LPCAT3 activity, but they cannot replace the complexity of the whole organisms or human disease in vivo.

This strategy should be applied to other LPCAT isoforms in the future to determine whether similar structural motifs are the basis of their different acyl-chain preferences and whether by making knock-in animal models with subtle tunnel or pocket mutations that can selectively affect positional selectivity, but not activity, activity. These models will then have to be combined with longitudinal studies of metabolic disease and inflammation and ferroptosis in liver and intestine to test whether pharmacological targeting of the side pocket of LPCAT3 can safely alter the content of arachidonoyl-PC, eicosanoid synthesis and ferroptotic susceptibility in clinically relevant conditions [19].

CONCLUSION

Fundamental Finding : This paper explains the mechanism by which LPCAT3 discriminates against incorporating arachidonoyl-CoA into phosphatidylcholine during phospholipid remodeling and the reason why this process is highly biased at the sn-2 site. A series of determinants in the acyl-donor tunnel and a hydrophobic side pocket, which selectively recognize the kinked structure of arachidonic acid, are identified using a combined method based on recombinant expression, quantitative kinetics, structure-guided mutagenesis, molecular modeling, and cell-based lipidomics. Predicted mutations in these areas disrupt arachidonoyl-CoA affinity, catalytic efficiency, and positional selectivity, suggesting that LPCAT3 is a stereochemical mould which matches substrate donors and acceptors to facilitate a successful sn-2 acyl transfer reaction. In line with this mechanism, the cells that express selectivity-impaired versions demonstrate decreased enrichment of arachidonoyl-PC species and reduced downstream outputs associated with the availability of arachidonates, such as stimulus-induced lipid mediator release and susceptibility to lipid peroxidation. Collectively, such results associate LPCAT3 structure with remodelling kinetics and with cellular arachidonoyl-

phospholipid homeostasis. **Implication :** This mechanistic structure will be used to support rational targeting of LPCAT3 to adjust membrane PUFA composition and associated phenotypes of inflammatory, metabolic, and ferroptotic types. **Limitation :** This paper explains the mechanism by which LPCAT3 discriminates against incorporating arachidonoyl-CoA into phosphatidylcholine during phospholipid remodeling and the reason why this process is highly biased at the sn-2 site. **Future Research :** This mechanistic structure will be used to support rational targeting of LPCAT3 to adjust membrane PUFA composition and associated phenotypes of inflammatory, metabolic, and ferroptotic types.

REFERENCES

[1] B. Wang and P. Tontonoz, "Phospholipid remodeling in physiology and disease," *Annu. Rev. Physiol.*, vol. 81, pp. 165–188, 2019, doi: 10.1146/annurev-physiol-020518-114444.

[2] M. A. Bermudez, J. M. Rubio, M. A. Balboa, and J. Balsinde, "Differential mobilization of the phospholipid and triacylglycerol pools of arachidonic acid in murine macrophages," *Biomolecules*, vol. 12, no. 12, p. 1851, 2022, doi: 10.3390/biom12121851.

[3] G. Shao *et al.*, "Research progress in the role and mechanism of LPCAT3 in metabolic related diseases and cancer," *J. Cancer*, vol. 13, no. 8, pp. 2430–2439, 2022, doi: 10.7150/jca.71619.

[4] A. S. Ali, S. K. Hachim, and Z. M. Saleh, "The role of IL-6 in inflammatory reaction during Coronavirus-19 infection: a review," *Int. J. Health Sci. (Qassim).*, 2022.

[5] C. Bartolacci *et al.*, "Targeting de novo lipogenesis and the Lands cycle induces ferroptosis in KRAS-mutant lung cancer," *Nat. Commun.*, vol. 13, no. 1, p. 4327, 2022, doi: 10.1038/s41467-022-31963-4.

[6] Y. Zhao *et al.*, "Identification and characterization of a major liver lysophosphatidylcholine acyltransferase," *J. Biol. Chem.*, vol. 283, no. 13, pp. 8258–8265, 2008, doi: 10.1074/jbc.M710422200.

[7] T. Hashidate-Yoshida *et al.*, "Fatty acid remodeling by LPCAT3 enriches arachidonate in phospholipid membranes and regulates triglyceride transport," *Elife*, vol. 4, p. e06328, 2015, doi: 10.7554/eLife.06328.

[8] X. Rong *et al.*, "Lpcat3-dependent production of arachidonoyl phospholipids is a key determinant of triglyceride secretion," *Elife*, vol. 4, p. e06557, 2015, doi: 10.7554/eLife.06557.

[9] I. Kabir, Z. Li, H. H. Bui, M.-S. Kuo, G. Gao, and X.-C. Jiang, "Small intestine but not liver lysophosphatidylcholine acyltransferase 3 (Lpcat3) deficiency has a dominant effect on plasma lipid metabolism," *J. Biol. Chem.*, vol. 291, no. 14, pp. 7651–7660, 2016, doi: 10.1074/jbc.M115.697011.

[10] Z. Li *et al.*, "Deficiency in lysophosphatidylcholine acyltransferase 3 reduces plasma levels of lipids by reducing lipid absorption in mice," *Gastroenterology*, vol. 149, no. 6, pp. 1519–1529, 2015, doi: 10.1053/j.gastro.2015.07.012.

[11] Q. Zhang *et al.*, "The structural basis for the phospholipid remodeling by lysophosphatidylcholine acyltransferase 3," *Nat. Commun.*, vol. 12, no. 1, p. 6869, 2021, doi: 10.1038/s41467-021-27244-1.

[12] H. Nakanishi *et al.*, "Cloning and characterization of mouse lung-type acyl-

CoA:lysophosphatidylcholine acyltransferase 1 (LPCAT1): Expression in alveolar type II cells and possible involvement in surfactant production," *J. Biol. Chem.*, vol. 281, no. 29, pp. 20140–20147, 2006, doi: 10.1074/jbc.M600225200.

[13] T. Harayama, H. Shindou, and T. Shimizu, "Biosynthesis of phosphatidylcholine by human lysophosphatidylcholine acyltransferase 1," *J. Lipid Res.*, vol. 50, no. 9, pp. 1824–1831, 2009, doi: 10.1194/jlr.M800500-JLR200.

[14] H. Shindou *et al.*, "A single enzyme catalyzes both platelet-activating factor production and membrane biogenesis of inflammatory cells: Cloning and characterization of acetyl-CoA:lyso-PAF acetyltransferase," *J. Biol. Chem.*, vol. 282, no. 9, pp. 6532–6539, 2007, doi: 10.1074/jbc.M609641200.

[15] R. Morimoto, H. Shindou, Y. Oda, and T. Shimizu, "Phosphorylation of lysophosphatidylcholine acyltransferase 2 at Ser34 enhances platelet-activating factor production in endotoxin-stimulated macrophages," *J. Biol. Chem.*, vol. 285, no. 39, pp. 29857–29862, 2010, doi: 10.1074/jbc.M110.147025.

[16] R. Morimoto, H. Shindou, M. Tarui, and T. Shimizu, "Rapid production of platelet-activating factor is induced by protein kinase Cα-mediated phosphorylation of lysophosphatidylcholine acyltransferase 2 protein," *J. Biol. Chem.*, vol. 289, no. 22, pp. 15566–15576, 2014, doi: 10.1074/jbc.M114.558874.

[17] D. Hishikawa, H. Shindou, S. Kobayashi, H. Nakanishi, R. Taguchi, and T. Shimizu, "Discovery of a lysophospholipid acyltransferase family essential for membrane asymmetry and diversity," *Proc. Natl. Acad. Sci. U. S. A.*, vol. 105, no. 8, pp. 2830–2835, 2008, doi: 10.1073/pnas.0712245105.

[18] X. Rong *et al.*, "LXRs regulate ER stress and inflammation through dynamic modulation of membrane phospholipid composition," *Cell Metab.*, vol. 18, no. 5, pp. 685–697, 2013, doi: 10.1016/j.cmet.2013.10.002.

[19] L. Yu *et al.*, "Review of Research Progress on Soil Moisture Sensor Technology," *Int. J. Agric. Biol. Eng.*, vol. 14, no. 4, pp. 32–42, 2021.

*__Ahmed Shakir Ahmed (Corresponding Author)__
Kirkuk Education Directorate General, Kirkuk, Iraq
Email: ahmed.aldoorii@gmail.com